

Enhanced light extraction from GaN based light-emitting diodes using a hemispherical NiCoO lens

Do-Hyun Kim,¹ Dong Su Shin,¹ and Jinsub Park^{1,2,*}

¹Department of Electronics and Computer Engineering, Hanyang University, Seoul 133-791, South Korea

²Department of Electronic Engineering, Hanyang University, Seoul 133-791, South Korea

*jinsubpark@hanyang.ac.kr

Abstract: We report on the improvement of light extraction efficiency from GaN-based light-emitting diodes (LEDs) using Ni_{1-x}Co_xO nanoparticles (NPs) formed on the p-GaN layer. After formation of Ni_{1-x}Co_xO hemispherical lens arrays on the blue LEDs by drop-casting colloidal NPs, electroluminescence (EL) and photoluminescence (PL) measurements are conducted to investigate the electrical and optical properties. The PL and EL intensities from the blue LEDs with the Ni_{1-x}Co_xO NPs are 1.74 and 1.61 times greater, respectively, than a conventional LED. Finally, a hybrid approach using ZnO nanorod arrays grown on the NiCoO hemispherical lens shows further increase of light extraction by 3.8 and 6.2 times compared to LEDs with bare NiCoO NPs and without any NPs, respectively. Finite-difference time-domain (FDTD) simulation results also agree well with the experimental results. The enhancement of light extraction from LEDs with ZnO nanorods and NiCoO NPs can be attributed to an enlarged escape angle cone and increased probability of light scattering.

©2014 Optical Society of America

OCIS codes: (160.6000) Semiconductor materials; (230.3670) Light-emitting diodes; (220.4241) Nanostructure fabrication.

References and links

1. S. Nakamura, T. Mukai, and M. Senoh, "Candela-class high-brightness InGaN/AlGaIn double heterostructure blue light emitting diodes," *Appl. Phys. Lett.* **64**(13), 1687–1689 (1994).
2. S. N. Mohammad, A. A. Salvador, and H. Morkoç, "Emerging gallium nitride based devices," *Proc. IEEE* **83**(10), 1306–1355 (1995).
3. Q. Zhang, K. H. Li, and H. W. Choi, "InGaIn light-emitting diodes with indium-tin-oxide sub-micron lenses patterned by nanosphere lithography," *Appl. Phys. Lett.* **100**(6), 061120 (2012).
4. Y. K. Ee, P. Kumnorkaew, R. A. Arif, H. Tong, H. Zhao, J. F. Gilchrist, and N. Tansu, "Optimization of light extraction efficiency of III-Nitride LEDs with self-assembled colloidal-based microlenses," *J. Select. Topics Quantum Electron.* **15**(4), 1218–1225 (2009).
5. S. H. Yeon and J. Park, "Enhancement of photoluminescence intensity of GaN-based light-emitting diodes with coated polystyrene/silica core-shell nanostructures," *J. Nanosci. Nanotechnol.* **13**(11), 7653–7657 (2013).
6. T. Son, K. Y. Jung, and J. Park, "Enhancement of the light extraction of GaN-based green light emitting diodes via nanohybrid structures," *Curr. Appl. Phys.* **13**(6), 1042–1045 (2013).
7. M. Khizar, Z. Y. Fan, K. H. Kim, J. Y. Lin, and H. X. Jiang, "Nitride deep-ultraviolet light-emitting diodes with microlens array," *Appl. Phys. Lett.* **86**(17), 173504 (2005).
8. L. E. Greene, M. Law, D. H. Tan, M. Montano, J. Goldberger, G. Somorjai, and P. Yang, "General route to vertical ZnO nanowire arrays using textured ZnO seeds," *Nano Lett.* **5**(7), 1231–1236 (2005).
9. F. Iacomi, G. Calin, C. Scarlat, M. Irimia, C. Doroftei, M. Dobromir, G. G. Rusu, N. Iftimie, and A. V. Sandu, "Functional properties of nickel cobalt oxide thin films," *Thin Solid Films* **520**(1), 651–655 (2011).
10. G. M. Kumar, D. H. Kim, and J. Park, "Colloidal Ni_{1-x}Co_xO nanostructures as anodic buffer layers in hybrid polypyrrole/Zn_{1-y}In_yO p-n junctions," *CrystEngComm* **15**(40), 8195–8201 (2013).
11. K. Song and J. Park, "Effects of the growth pressure of a-plane InGaIn/GaN multi-quantum wells on the optical performance of light-emitting diodes," *Semicond. Sci. Technol.* **28**(1), 015010 (2013).

12. C. F. Windisch, Jr., G. J. Exarhos, K. F. Ferris, M. H. Engelhard, and D. C. Stewart, "Infrared transparent spinel films with p-type conductivity," *Thin Solid Films* **398-399**, 45–52 (2001).
13. X. Li, X. Zhang, Z. Li, and Y. Qian, "Synthesis and characteristics of NiO nanoparticles by thermal decomposition of nickel dimethylglyoximate rods," *Solid State Commun.* **137**(11), 581–584 (2006).
14. L. H. Ai and J. Jiang, "Rapid synthesis of nanocrystalline Co₃O₄ by a microwave-assisted combustion method," *Powder Technol.* **195**(1), 11–14 (2009).
15. T. S. Kim, S. M. Kim, Y. H. Jang, and G. Y. Jung, "Increase of light extraction from GaN based light emitting diodes incorporating patterned structure by colloidal lithography," *Appl. Phys. Lett.* **91**(17), 171114 (2007).
16. C. F. Windisch, K. F. Ferris, and G. J. Exarhos, "Synthesis and characterization of transparent conducting oxide cobalt–nickel spinel films," *J. Vac. Sci. Technol.* **19**(4), 1347–1351 (2001).
17. J. K. Kim, A. N. Noemaun, F. W. Mont, D. Meyaard, E. F. Schubert, D. J. Poxson, H. S. Kim, C. Sone, and Y. J. Park, "Elimination of total internal reflection in GaInN light-emitting diodes by graded refractive-index micropillars," *Appl. Phys. Lett.* **93**(22), 221111 (2008).
18. M. K. Lee, C. L. Ho, and P. C. Chen, "Light extraction efficiency enhancement of GaN blue LED by liquid-phase-deposited ZnO Rods," *IEEE Photon. Technol. Lett.* **20**(4), 252–254 (2008).
19. Z. Yin, X. Liu, H. Wang, Y. Wu, X. Hao, Z. Ji, and X. Xu, "Light transmission enhancement from hybrid ZnO micro-mesh and nanorod arrays with application to GaN-based light-emitting diodes," *Opt. Express* **21**(23), 28531–28542 (2013).
20. Y. H. Ko and J. S. Yu, "Urchin-aggregation inspired closely-packed hierarchical ZnO nanostructures for efficient light scattering," *Opt. Express* **19**(27), 25935–25943 (2011).
21. Z. Yin, X. Liu, H. Wang, Y. Wu, X. Hao, Z. Ji, and X. Xu, "Light transmission enhancement from hybrid ZnO micro-mesh and nanorod arrays with application to GaN-based light-emitting diodes," *Opt. Express* **21**(23), 28531–28542 (2013).

1. Introduction

GaN-based nitride compound semiconductors are very attractive materials due to their superior material properties and their versatility for use in a variety of optoelectronic applications such as light-emitting diodes (LEDs), solar cells, and laser diodes [1]. In particular, III-nitride based LEDs have been considered as a candidate of next generation solid-state light sources for replacement of general lighting sources such as florescent lamps due to their environmentally friendly properties and long lifetime (~40,000 hrs) [2]. Currently, the internal quantum efficiency of GaN-based LEDs can exceed 90%, but the external quantum efficiency is relatively low due to total internal reflection (TIR) of the generated light at the nitride-air interface resulting from their very different refractive indices [3, 4]. Many novel methods have been suggested for enhancing light extraction of LEDs using nanoparticles, nanowires/nanorods, and various types hemispherical lenses formed on the LED surface [5–7]. Of the nanomaterials reported for the improvement of light extraction from LED, zinc oxide (ZnO) is one of the most frequently used semiconductor materials due to its relatively low production cost and superior optical properties [8]. In this study, we investigated the effects of, particularly the improvement of light extraction efficiency, a newly suggested combination of NiCoO nanoparticles (NPs) together with ZnO nanorod arrays, formed on the p-GaN layer of blue LEDs. NiCoO is a representative p-type material consisting of NiO and CoO, which can be a candidate material to replace indium tin oxide (ITO) as a transparent conducting layer in visible range due to the similar material properties [9]. Significant improvements in light extraction from blue LEDs are achieved by the use of bare NiCoO NPs and combination of ZnO nanorod arrays and NiCoO NPs. A theoretical analysis is conducted using finite-difference time-domain (FDTD) simulations and those results agree well with the experimental results.

2. Experimental details

A solution-based synthesis was used to obtain NiCoO NPs; the raw materials were Ni(II) acetate tetrahydrate(98.0%), Co(II) acetate tetrahydrate(98.0%), and KOH potassium hydroxide(85.0%). The initial stock solutions were made with 150 mL deionized (DI) water, dissolving the nickel acetate- and cobalt acetate-based salts in a 70:30 weight ratio. The metallic precursor homogeneity was achieved by simply stirring the stock solutions continuously for 48 hrs prior to the precipitation reactions. The stock solutions were then

treated with drops of 10 M KOH until precipitation ceased. The details for the NiCoO NP synthesis can be found in other reference [10]. After synthesis of NiCoO, the NPs are drop-casted onto the surface of GaN-based LED epi structures grown by metal organic chemical vapor deposition (MOCVD) [11]. Finally, ZnO nanorod arrays are formed on top of the NiCoO NPs using the hydrothermal method [6]. Photoluminescence (PL) and electroluminescence (EL) measurements were conducted to determine the effects of the NiCoO NPs and the ZnO nanorod arrays on the light extraction efficiency in LEDs.

3. Results and discussion

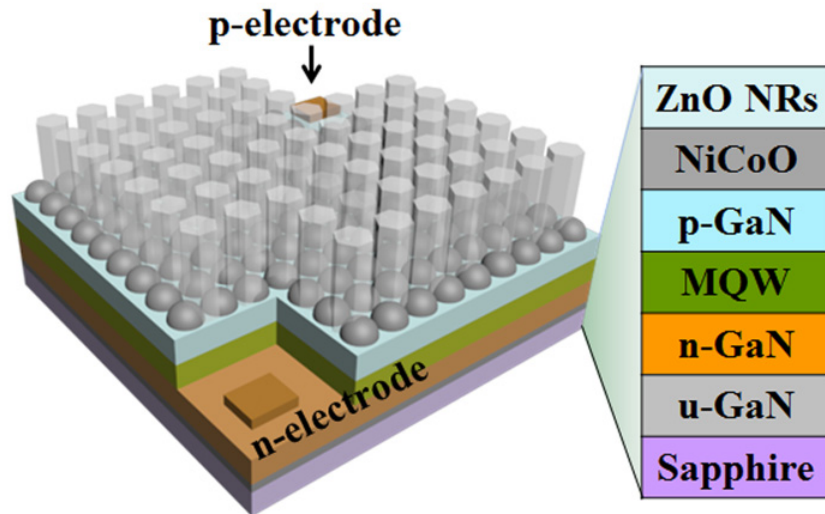


Fig. 1. Schematic diagram of fabricated blue LED structures with ZnO nanorod arrays on $\text{Ni}_{1-x}\text{Co}_x\text{O}$ hemispherical lenses.

Figure 1 shows a schematic diagram of a blue LED structure with the NiCoO NP hemispherical lenses and ZnO nanorod arrays formed on the top-most layer. The layer structure of the blue LEDs with 450 nm emission was grown by MOCVD on c-plane Al_2O_3 substrates. After coating the NiCoO NPs on p-GaN layer, ZnO nanorod arrays are formed on top of the NiCoO hemispherical lens. Before the formation of p-electrode on p-GaN, the NiCoO NPs are partially removed.

To confirm the formation of the NiCoO NPs, x-ray diffraction (XRD) and transmission electron microscopy (TEM) measurements were conducted. Figure 2(a) shows the powder XRD patterns obtained from the synthesized NiCoO NPs. The XRD spectrum clearly reveals diffraction peaks attributable to face-centered cubic structured NiO related to the (111), (220), (311), and (222) crystal planes (JCPDS 73-1523). The secondary material peaks were from Co_3O_4 , corresponding to the (220), (511), and (440) crystal planes (JCPDS 78-1970). Figure 2(b) shows TEM images of the synthesized nickel-cobalt oxide particles. As shown in the image, the average size of NiCoO is approximately 15 nm, which can be adjusted by the specifics of the synthesis method.

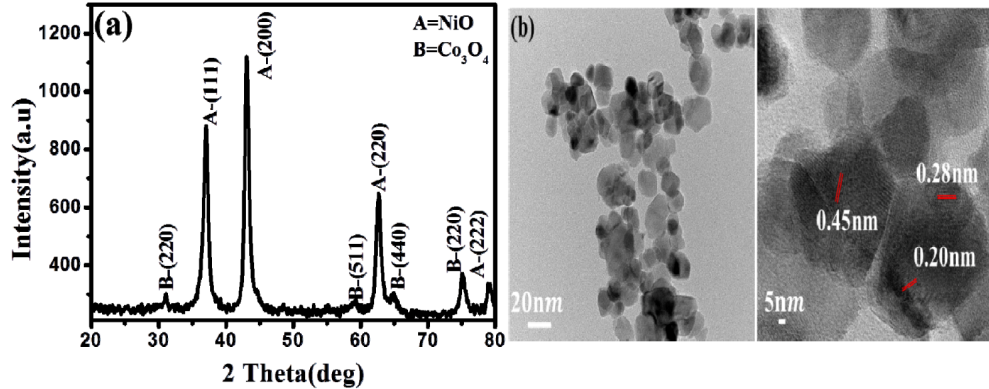


Fig. 2. (a) Powder XRD patterns and plane indices of the A(NiO) and B(Co₃O₄) phase in Ni_{1-x}Co_xO NPs. (b) TEM images of the Ni_{1-x}Co_xO NPs at low magnification (left) and high magnification (right)

To evaluate the optical properties of the NiCoO NPs, UV-Vis absorption measurements are conducted. The UV-Vis spectrum obtained from the NiCoO NPs reveals an absorption band edge with an intensity maximum centered around 300 nm, as shown in Fig. 3. Although there is a shift in absorption band edge by ligand–metal charge transfer processes [12], absorption bands are observed at 320 and 280 nm for the NiO and Co₃O₄ phases, respectively [13, 14]. Furthermore, the optical band gap

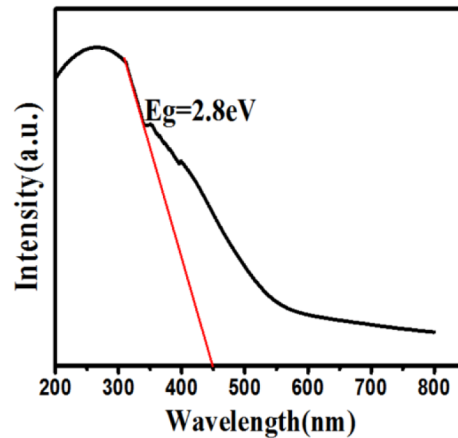


Fig. 3. UV-Vis absorbance spectrum of the colloidal Ni_{1-x}Co_xO dispersions in solvent.

of the synthesized oxide nanomaterial was extrapolated to be approximately 2.8 eV (442 nm) which indicates that the synthesized NiCoO NPs can be used as a transparent oxide layer in the visible range.

In order to investigate the morphology of the NiCoO NPs and ZnO nanorod arrays formed on p-GaN layer, scanning electron microscope (SEM) observations are performed. Figures 4(a) and 4(b) show SEM image of the NiCoO NP hemispheres formed on the p-GaN layer and a distribution of the nanoparticle sizes, respectively. A drop-casting method was used to form the NiCoO hemispherical lens. The SEM image shows that the hemisphere-type NiCoO NPs are uniformly distributed on the surface. From the SEM images, the average surface coverage and diameter of NPs on LED surface were measured as 50–60% and 73 nm, respectively. After formation of the NiCoO hemispherical lenses on the LED top surface, the

ZnO nanorod arrays are formed on NiCoO NP coated LEDs by the hydrothermal synthesis method [6].

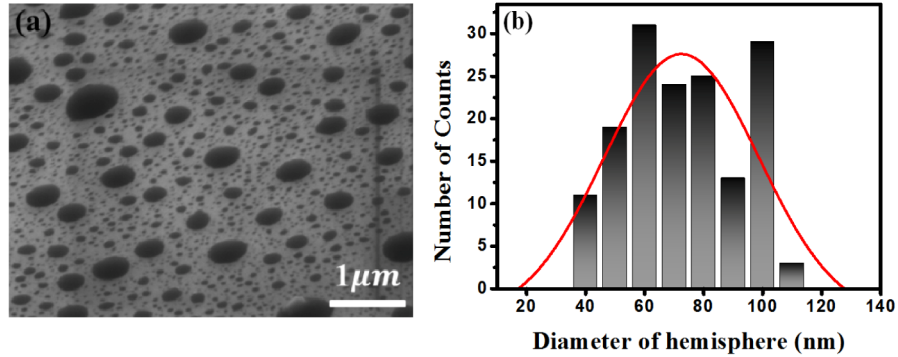


Fig. 4. (a) SEM image of $\text{Ni}_{1-x}\text{Co}_x\text{O}$ hemisphere lens coated on top of p-GaN. (b) The histogram for the diameter distribution of hemispherical NiCoO NPs.

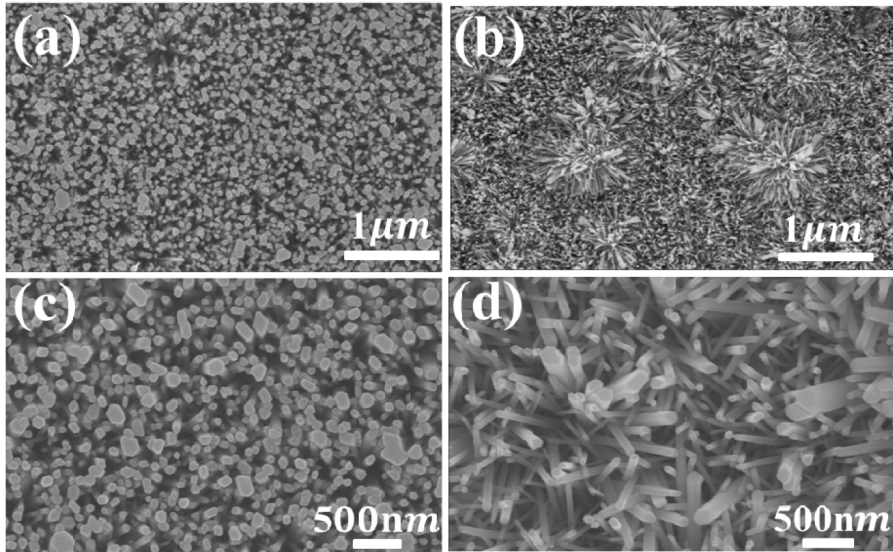


Fig. 5. SEM images obtained from the ZnO nanorod arrays on (5(a) and 5(c)) a conventional LED and (5(b) and 5(d)) a NiCoO NP/LED. (c) and (d) show magnified SEM images for 5(a) and 5(b), respectively.

Figures 5(a) and 5(b) show ZnO nanorod arrays formed on a conventional blue LED and on a NiCoO NP coated LED, respectively. ZnO nanorods grown using a general hydrothermal growth condition (6 h at 95°C) show an average diameter and length of 60 nm and 1 μm, respectively. Figures 5(c) and (d) show magnified images of Figs. 5(a) and 5(b), respectively. Although some deviation of direction occurred in the ZnO nanorod arrays grown on top of the NiCoO NPs, all samples show vertically aligned nanorod morphology along the growth direction of the GaN LED epi structures. The formation of NiCoO NPs effects on the growth of ZnO nanorods due to its spherical shape.

To investigate the effects of NiCoO hemispherical lens coatings on the surface of LEDs on the light extraction properties from blue LEDs, PL measurements are conducted using a 325 nm He-Cd excitation source at room temperature. Figure 6 shows the PL spectra of the uncoated and NiCoO NP-coated LED samples, whose emission peak wavelength was approximately 450 nm in all samples. The integrated PL luminescence intensity for LEDs

with the hemispherical NiCoO lens arrays showed a 1.8-fold enhancement over that of the uncoated sample. Generally, in the case of GaN-based LEDs, the large refractive index difference between GaN ($n = 2.5$) and air ($n = 1$) makes it quite difficult for photons to escape from the nitride to air.

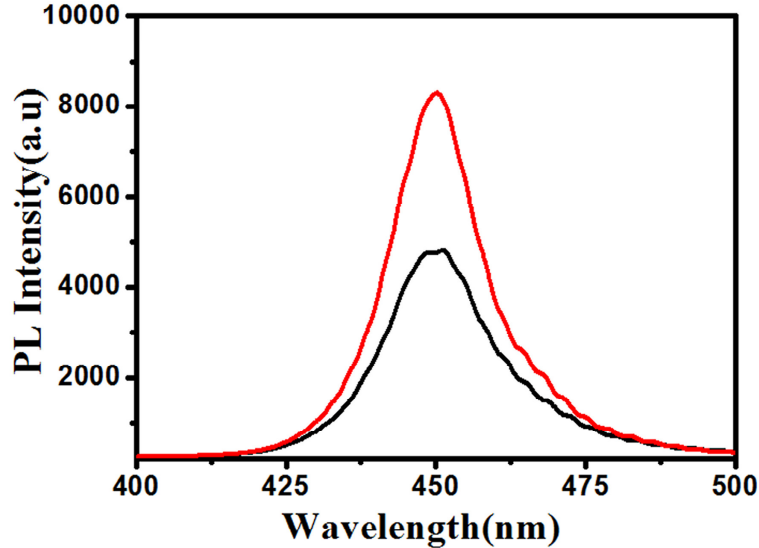


Fig. 6. The PL spectra of the LEDs with (red line) and without (black line) NiCoO hemisphere lens formed on top of p-GaN .

Specifically, the escape cone angle is very narrow, which means that due to total internal reflection, most of the light generated by the active regions is trapped in the higher refractive index semiconductor material [15]. The improvement of light extraction in LED with NiCoO hemisphere array can be attributed to the effects of the graded refractive index. The refractive index of NiCoO is 1.7, intermediate value between those of GaN and air, which results in an enlargement of the escape cone and a corresponding increase of light scattering probability in the NPs [16, 5].

EL measurements are conducted at various injection current levels to show the effects of NiCoO NPs as well as that of the combined ZnO nanorod and NiCoO NP structures on the light extraction in blue LED with turn-on status. The EL spectra for the various surface nano structured blue LEDs (bare ZnO nanorods, bare NiCoO NPs, ZnO nanorods/NiCoO NPs) under an injection current fixed at 50 mA are shown in Fig. 7. The EL intensity of LEDs with ZnO nanorod/NiCoO NPs is the highest. The integrated EL intensity of the samples covered with hemispherical NiCoO lenses and ZnO nanorod/NiCoO hemispherical arrays exhibited enhancements of 1.6 and 6.1 times, respectively, over that of the uncoated sample. EL intensity measurements were also conducted on LEDs with bare ZnO nanorods, which are generally used to make nanohybrid structures. Although the ZnO nanorods/LED structure shows a higher EL intensity than the NiCoO NPs/LED structure did, the combined ZnO nanorods/NiCoO NPs/LED structure showed a 20% further increase in EL intensity over LEDs with bare ZnO nanorods. The increase of light extraction efficiency in blue LEDs with the ZnO nanorod/NiCoO NP structures can be explained by a similar mechanism to that used for the PL intensity enhancement displayed in Fig. 6.

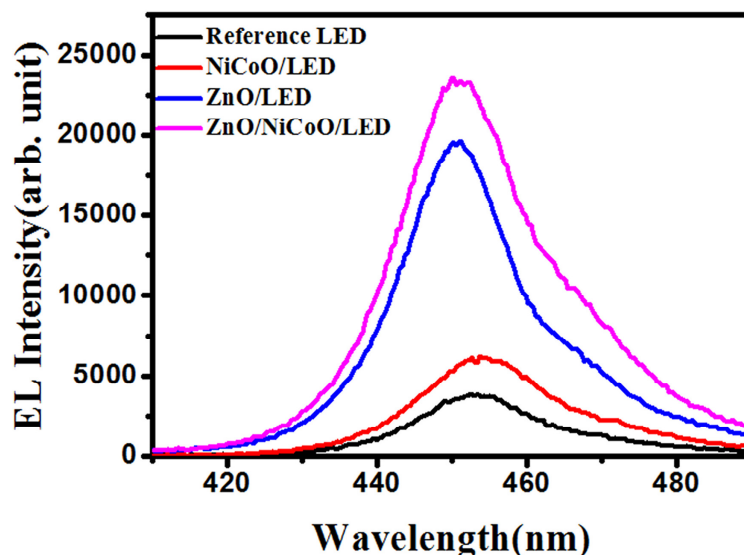


Fig. 7. EL spectra obtained from blue LEDs with different surface nanostructures at an injection current of 50mA.

The enhancement in light extraction from LEDs can be attributed to the enlarged effective photon escape cone by the NiCoO hemisphere lens arrays, and additional reduced Fresnel reflections at the surface due to a gradual change of refractive indices at, respective, the air/ZnO nanorod/NiCoO NP/GaN interfaces [17,18]. In addition, the use of ZnO nanorods on NiCoO hemispheres further enhances the light interference and diffusing properties which may act on the diffusion center resulting in improvement of the light extraction [19, 20].

Finally, for the theoretical consideration of the relationship between various nanostructure formation and light extraction from LEDs, FDTD simulations are conducted using a Lumerical simulation method. A single polarized dipole source is located at the center of the InGaN quantum well active layer, and both the detection plane and line are placed over the top surface of the LEDs. The LED structures and the sizes of NiCoO hemisphere and ZnO nanorods used in the FDTD simulation are approximately similar to those used in our experiments. The light emission output was measured in the top-view direction of the LED structures. The simulated results for the electric field intensity, as an indication of light extraction are shown in Fig. 8. Figures 8(a)-8(d) indicate the spatial distribution of extracted light intensity for LEDs with the different nanostructures, as denoted in the Fig. 8. The integrated intensity values are indicated by the round dots in figure with respect to sample name. As in the experimental results, the ZnO nanorod/NiCoO NP/LED structure shows highest light extraction efficiency compared to the other LED structures. FDTD simulation results show that the improvement of light extraction was achieved by using the NiCoO hemispherical lenses and the combination of ZnO nanorod arrays on NiCoO NP. The blue LEDs with ZnO nanorod arrays on NiCoO NPs show a 10.9-fold light extraction improvement over LEDs without any nanostructures. For the bare NiCoO NPs formed on the LED surface, the light extraction intensity increased by 1.37 times over the reference LED. The simulation results were in good agreement with the experimental results.

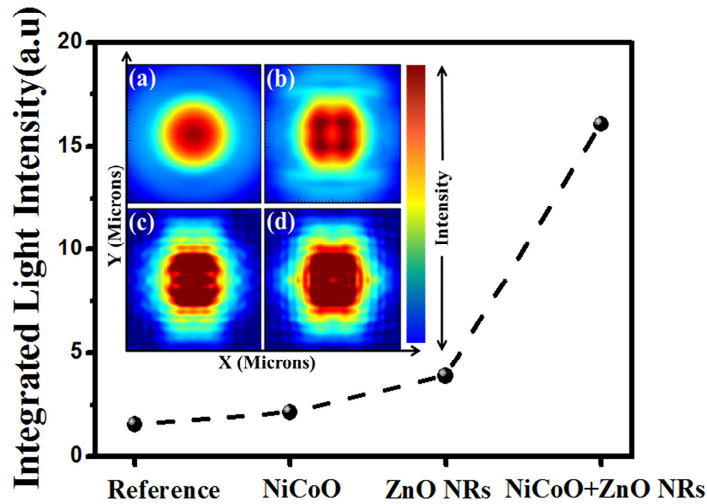


Fig. 8. FDTD simulation results for light extraction characteristics as a function of various different nanostructures.

4. Conclusions

In summary, we report on the improvement of light extraction from blue LEDs using NiCoO hemispherical lens arrays both alone and in a hybrid structure with ZnO nanorods. EL intensity of the LED with the hemispherical NiCoO lens was 1.61 times greater than the reference LEDs. In addition, the combined hybrid structure with ZnO nanorod arrays formed on top of the hemispherical NiCoO lenses show a further improvement in light extraction, approximately 6.5 times greater than the LED without nanomaterials. The experimentally measured results are entirely consistent with FDTD simulations, and the improvements in photon extraction can be attributed to the enlarged escape angle and reduction of Fresnel reflection loss due to the use of NiCoO and ZnO materials whose refractive indices are located between those of GaN and air.

Acknowledgments

This research was supported by the Basic Science Research Program through the National Research Foundation of Korea (NRF-2012R1A1A1041930) and the BK21 PLUS(Brain Korea 21 Program for Leading Universities & Students), funded by the Ministry of Education, Science and Technology.